Biophysical Journal, Volume *115*

Supplemental Information

Effect of Substrate Stiffness on Mechanical Coupling and Force Propagation at the Infarct Boundary

Dung Trung Nguyen, Neerajha Nagarajan, and Pinar Zorlutuna

Effect of Substrate Stiffness on Mechanical Coupling and

Force Propagation at the Infarct Boundary

T.D. Nguyen, N. Nagarajan, P. Zorlutuna*

Supporting Material

Porohyperelastic (PHE) field theory

PHE theory has developed as an extension of the poroelastic theory [1] to characterize and predict large deformations and non-linear responses in structures under loading. This theory assumes the cell as a continuum material consists of an incompressible fluid saturated in an incompressible hyperelastic porous solid. While the solid and fluid are incompressible, the whole cell is compressible due to fluid loss during deformation.

The PHE constitutive law requires two material properties including the drained effective strain energy density function, W^e, and the hydraulic permeability, $\tilde{k}_{ij}$. W^e defines the "effective" Cauchy stress, σ_{ij}^e, as:

$$\sigma_{ij} = \sigma_{ij}^e + \pi^f \delta_{ij}, \quad \sigma_{ij}^e = J^{-1} F_{im} S_{mn}^e F_{jn} \tag{3}$$

$$S_{ij} = S_{ij}^e + J\pi^f H_{ij}, \quad H_{ij} = F_{im}^{-1} F_{jm}^{-1}, \quad S_{ij}^e = \frac{\partial W^e}{\partial E_{ij}} \tag{4}$$

where π^f is the pore fluid stress = – (pore fluid pressure); S_{ij}^e, and H_{ij} are second Piola-Kirchhoff stress, and Finger's strain, respectively.

Conservation of fluid mass (Darcy's law):

$$\tilde{k}_{ij} \frac{\partial \pi^f}{\partial X_i} = \dot{\tilde{w}}_j \tag{5}$$

For simplicity, the Neo-Hookean hyperelastic material model is used in this study [2, 3] with strain energy density function shown below:

$$W^e = C_1(\bar{I}_1 - 3) + \frac{1}{D_1}(J-1)^2 \tag{6}$$

where $\bar{I}_1 = J^{-2/3} I_1$ is the first deviatoric strain invariant, and C_1 and D_1 are material constants.

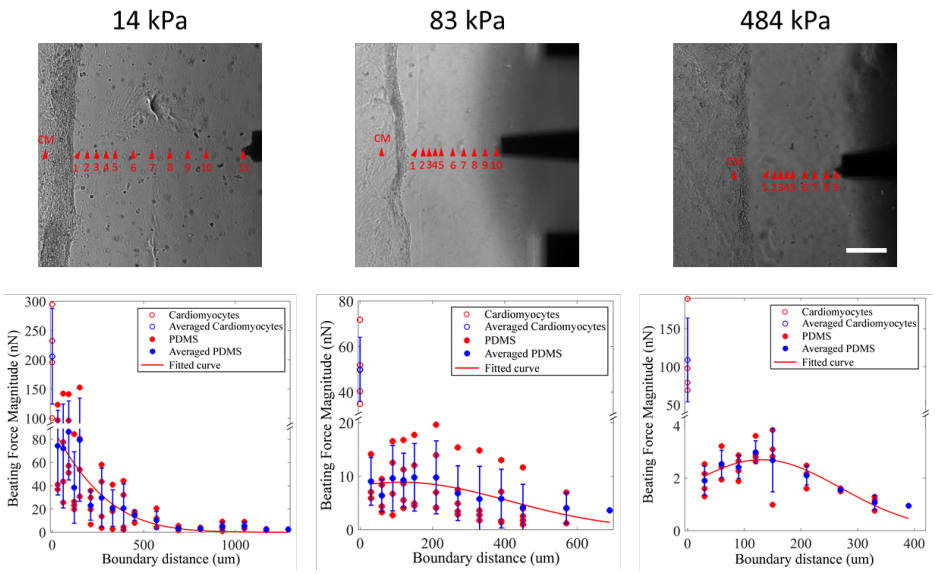

Figure S-1. Mechanical signal propagation at the CM-PDMS boundary on the control samples without any CMFs. Top: Brightfield images of soft, middle and stiff substrates samples (from left to right). The red arrowheads indicated the tested locations for each sample. Bottom: Beating force magnitude (nN) versus boundary distance (μm) curves of the samples. Scale bars: 100 μm.

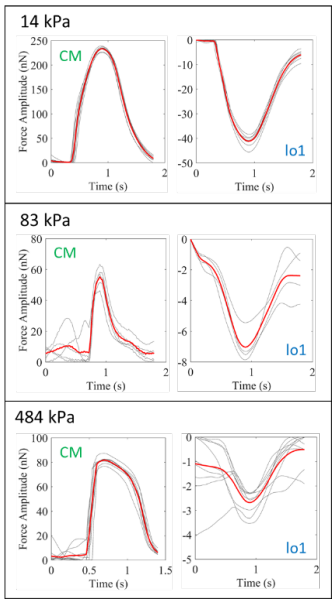

Figure S-2. Representative images of contractile force patterns at the CM-PDMS boundary for the control samples without any CMFs for soft, middle and stiff substrates (from top to bottom).

Cardiomyocytes (CMs) beating angle calculation

In this study, a customized image processing code was developed using MATLAB (The MathWorks, Inc.) to calculate CMs contracting angle. Briefly, images at relaxed and most contracted stages of CMs were first extracted from brightfield videos. Identical features from these images were then detected and shown as red circles and green crosses (Figure S-3) for relaxed and contracted stages, respectively. CMs beating angle was calculated as the angle α of a connected line between a red circle and a green cross (insert image in Figure S-3) measured from a horizontal axis (i.e. the reference line). The positive direction of the reference line was always directed to the CMs region. The angle was positive or negative when it was in clockwise or counter-clockwise direction with respect to the reference line, respectively. Note that only features located at similar coordinates with

the probe, where the measurements were performed, were selected for contractile angle calculation (white circle in Figure S-3). Beating angles corresponding to beating patterns of CM-CMF and CM-PDMS samples for soft, middle and stiff substrates are shown in Table S-1 to S-3, respectively.

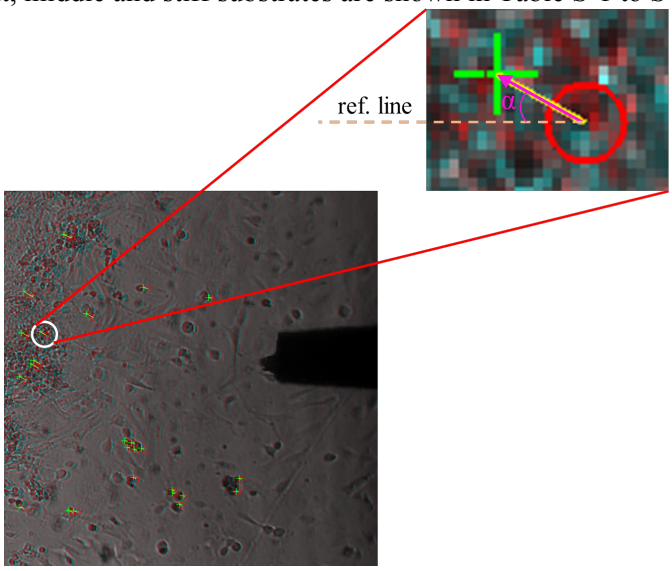

Figure S-3. Brightfield image of a soft substrate CM-CMF sample showing identical feature locations at relax (red circles) and most contracted (green crosses) stages of CMs. The white circle indicates the feature locations used for CMs beating angle calculation; Insert: Zoom-in image of the white circle showing how to calculate CMs contractile angle α.

Table S-1. Beating angle corresponding to beating pattern of soft substrate CM-CMF and CM-PDMS samples

Sample No.		S1	S2	S3	S4	S5	AVG
CM-CMF	Beating pattern				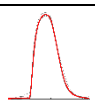		
	Beating angle α (^{0})	29.45	29.38	9.18	13.54	8.60	18.03
CM-PDMS	Beating pattern						
	Beating angle α (^{0})	-21.91	11.94	15.55	-17.83		-3.06

Table S-2 Beating angle corresponding to beating pattern of moderate substrate CM-CMF and CM-PDMS samples

Sample No.		S1	S2	S3	S4	S5	S6	AVG
CM-CMF	Beating pattern	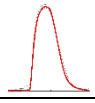		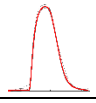		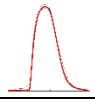	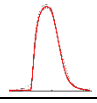	
	Beating angle α (^{0})	-21.60	-1.20	65.83	58.07	13.06	-46.86	20.17
CM-PDMS	Beating pattern							
	Beating angle α (^{0})	7.92	25.00	20.48	-29.43			5.99

Table S-3 Beating angle corresponding to beating pattern of stiff substrate CM-CMF and CM-PDMS samples

Sample No.		S1	S2	S3	S4	S5	S6	S7	AVG
CM-CMF	Beating pattern								
	Beating angle α (^{0})	17.10	-7.95	22.07	88.07	30.16	-22.52	12.42	19.91
CM-PDMS	Beating pattern								
	Beating angle α (^{0})	-33.48	22.62	25.89	-9.71				1.33

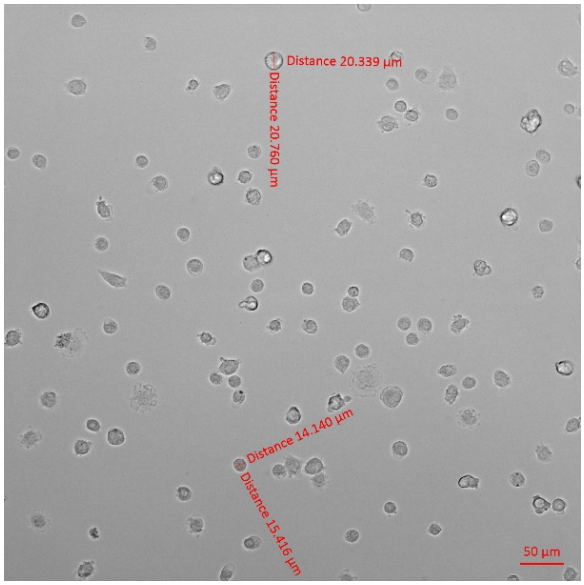

Figure S-4. Brightfield image of CMFs seeded on petri dish for 15 mins. Diameter of a cell was calculated as average of 2 diagonal diameters as shown by 2 red lines. Scale bar: 50 µm.

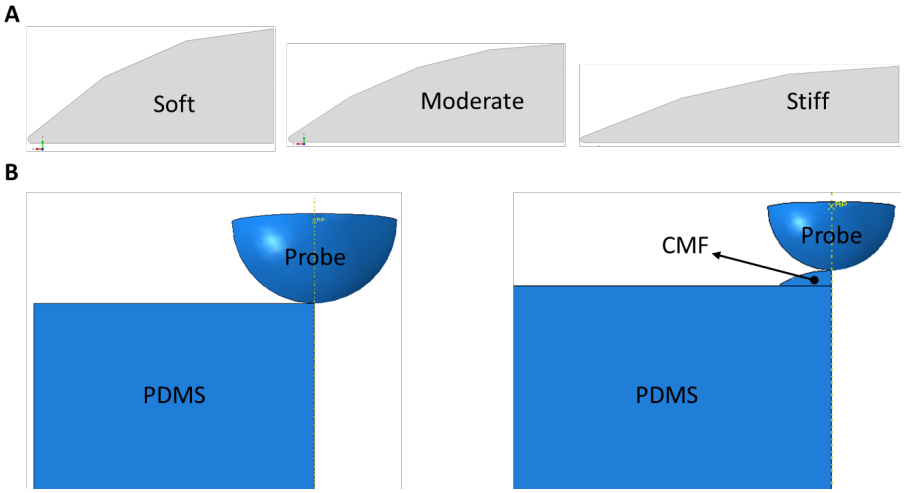

Figure S-5. FEA indentation models of PDMS substrates and CMFs. (A) CMFs' models when seeded on soft, middle and stiff substrates showing different degree of spreading. (B) Left panel: FEA indentation model of a PDMS substrate. Right panel: FEA indentation model of CMF seeded on a PDMS substrate.

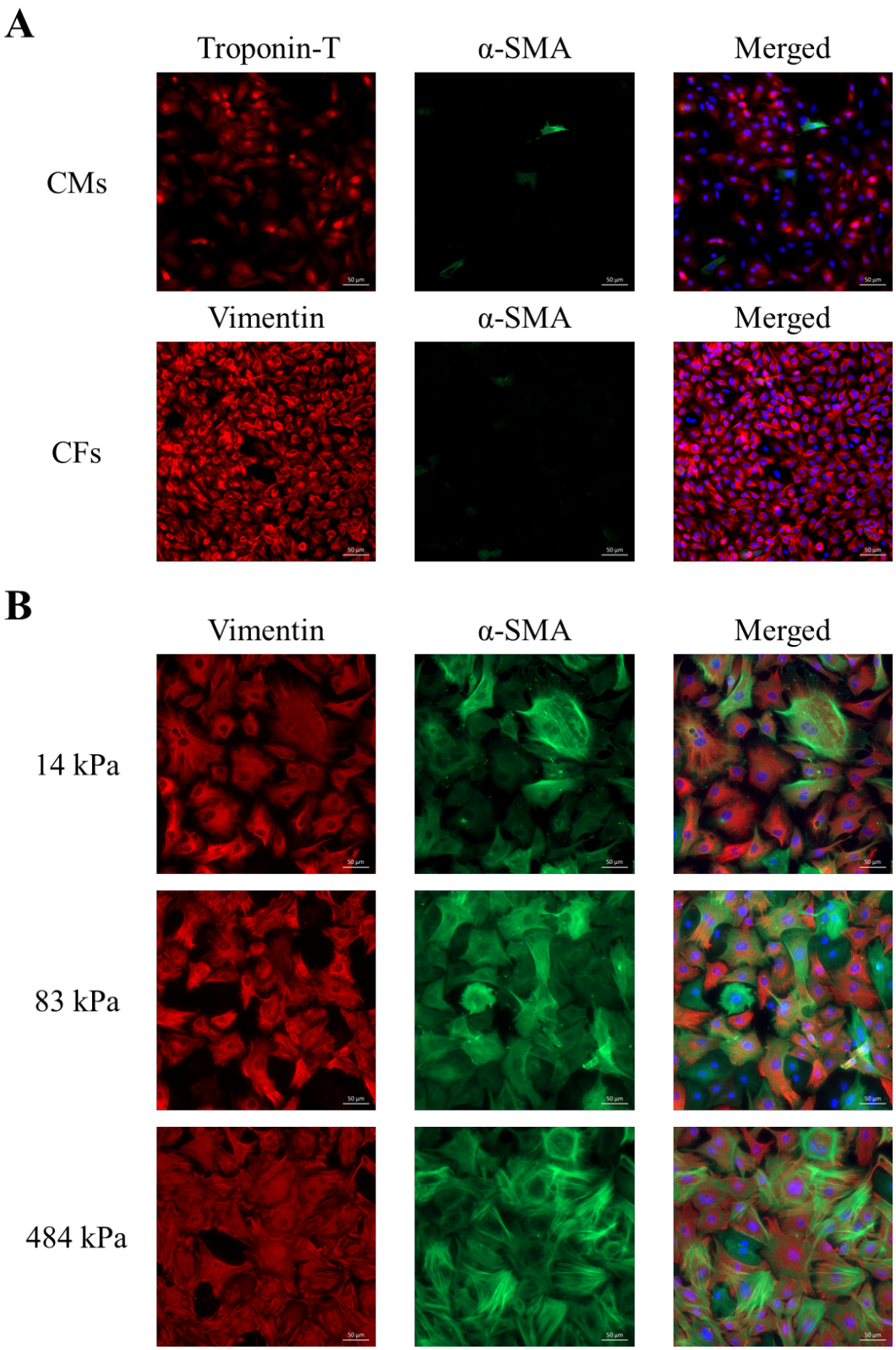

Figure S-6. A) Immunostaining of CMs and CFs on Day 1 after cell isolation. Top: CMs samples were stained with Troponin-T (red) and α- smooth muscle actin (SMA) (green). Bottom: CFs samples were stained with Vimentin (red) and α- smooth muscle actin (SMA) (green) (B) Biochemical characterization of Vimentin (red) and α- smooth muscle actin (SMA) (green) on soft, moderate and stiff samples on Day 5. Cell nuclei were counterstained with DAPI (blue) in all samples. (Scale bars: 50 μm).

Table S-4 The FEA simulation material constants of the PHE models.

		Simulation material constants			
		C1 (kPa)	*D1* (1/kPa)	k_0 (10^8 $\mu m^4/N.s$)	*v*
Unseeded PDMS substrates and native tissues	Soft substrate	3.41	0.124	253.84	0.31
	Moderate substrate	19.50	0.017	94.17	0.35
	Stiff substrate	96.50	0.00085	14.74	0.46
CMFs seeded on PDMS substrates	Soft substrate	0.35	8.4	0.61	-0.24
	Moderate substrate	0.48	4.8	0.61	-0.15
	Stiff substrate	0.38	6	0.82	-0.15

Table S-5 Simulation results showing the different beating waveform patterns and varying force magnitudes (nN) experienced by the CMF due to beating of an adjacent CM with different cell-cell and cell-substrate interaction profiles. Both effects of CMF and substrate stiffness were considered. Note that the CM stiffness was kept constant at 1.5 kPa in all simulations.

Substrate stiffness	CMF stiffness	With cell-matrix adhesion at cell-cell interface		Without cell-matrix adhesion at cell-cell interface	
		Pattern	Magnitude (nN)	Pattern	Magnitude (nN)
Soft (14 kPa)	1 kPa	"beating"	0.011	"pulling"	0.329
	1.5 kPa	"beating"	0.022	"pulling"	0.558
	2 kPa	"beating"	0.031	"pulling"	0.589
Moderate (83 kPa)	1 kPa	"beating"	0.013	"pulling"	0.328
	1.5 kPa	"beating"	0.024	"pulling"	0.557
	2 kPa	"beating"	0.034	"pulling"	0.588
Stiff (484 kPa)	1 kPa	"beating"	0.013	"pulling"	0.328
	1.5 kPa	"beating"	0.024	"pulling"	0.557
	2 kPa	"beating"	0.035	"pulling"	0.588

Supporting Movie S-1. Ca^{2+} flux video of a co-culture sample on a stiff substrate.

Supporting Movie S-2. Brightfield video of contracting CMs stretching CMFs on a soft substrate

References

[1] B.R. Simon, M.A. Gaballa, Total Lagrangian 'porohyperelastic' finite element models of soft tissue undergoing finite strain.pdf, 1989 advances in bioengineering, B Rubinsky (ed) BED-vol 15, ASME, New York (1989) 97-98.
[2] C.P. Brown, T.C. Nguyen, H.R. Moody, R.W. Crawford, A. Oloyede, Assessment of common hyperelastic constitutive equations for describing normal and osteoarthritic articular cartilage, Proceedings of the Institution of Mechanical Engineers, Part H: Journal of Engineering in Medicine 223(6) (2009) 643-652.
[3] ABAQUS, ABAQUS/Standard User's Manual (version 5.6), Hibbitt, Karlsson, and Sorensen, Inc., Pawtucket, USA, 1996.